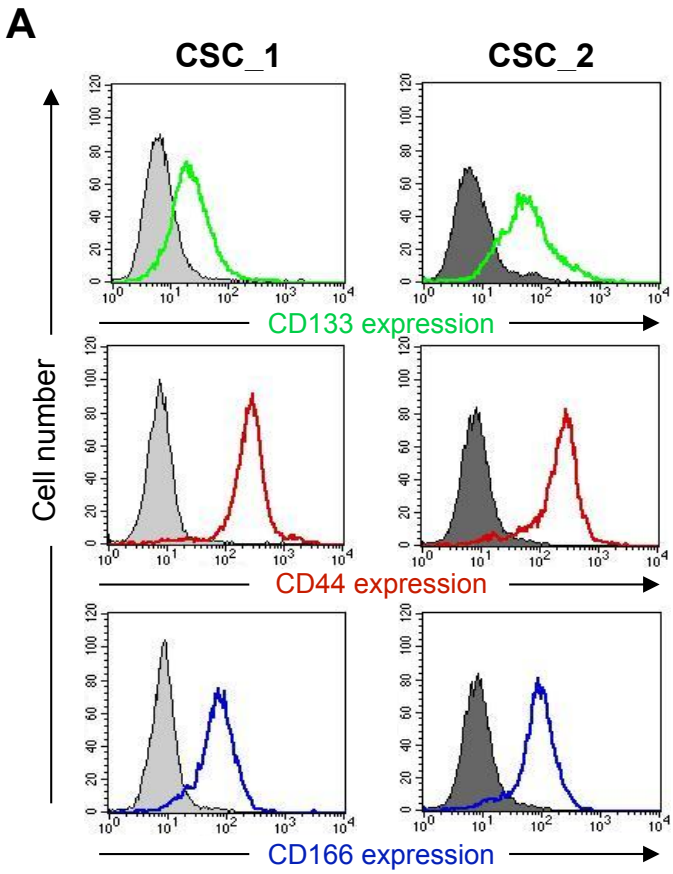


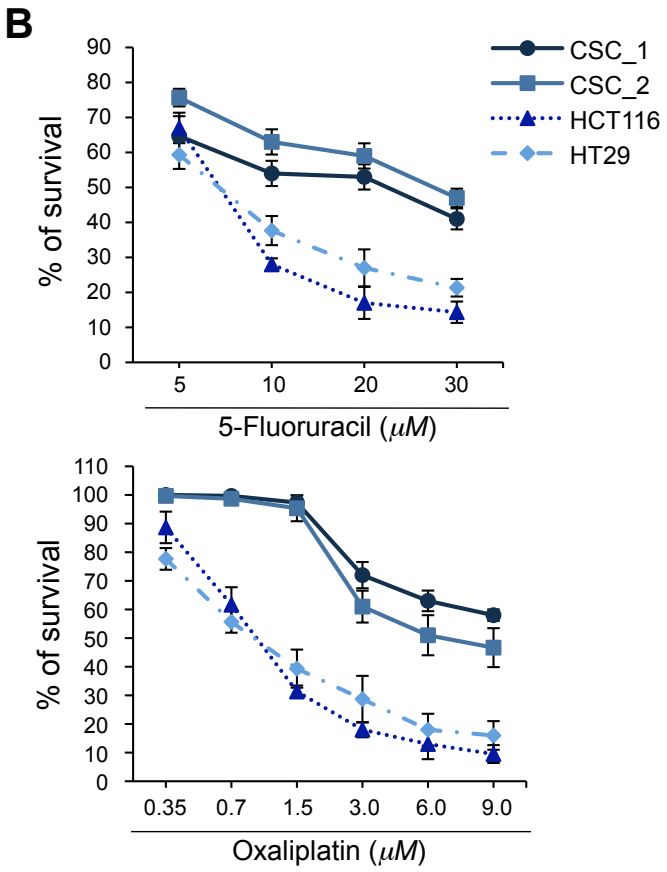


C

| | TUMOR TAKE | DAYS OF TUMOR APPEARENCE | TUMOR WEIGHT *(day 25 p.i.)* |
|---|---|---|---|
| **HCT116** | 5/5 | 3,3,4,4,4 | 196 ± 62 |
| **CSC_1** | 4/5 | 11,11,14,22 | 131 ± 44 |

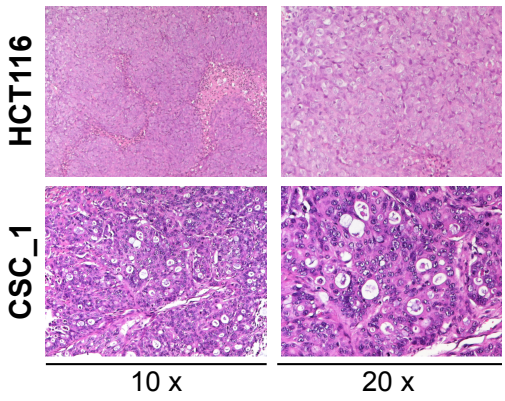


**Supplemental Figure S1.** Characterization of patient derived colon CSCs. **A** Evaluation of CD133 (upper panel), CD44 (middle panel) and CD166 (lower panel) expression by FACS analysis. Histograms represent the fluorescence intensities of each of the three markers (colored lines) in two patient-derived colon CSCs (CSC_1 and CSC_2). Analyses of negative controls (gray areas) are shown. **B** Colon CSCs, HCT116 (ATCC) and HT29 (ATCC) cells were treated for 96 hrs with the indicated doses of 5-Fluoruracil (upper panel) or Oxaliplatin (lower panel) and colony forming ability was evaluated. The histograms show the surviving fractions calculated as the ratio of absolute survival of the treated sample/absolute survival of the control sample. **C** Colon CSC_1 and HCT116 were injected subcutaneously in immunosuppressed mice at $10^6$ cells/mouse and tumor take and growth were evaluated. **D** Representative Immunohistochemistry (IHC) images from C. Tumors were excised from mice, embedded in paraffin, stained with Haematoxylin-Eosin and then analyzed by light microscopy (AxioCam MRc 5) on 2-3 μm microtome sections. Morphological analysis shows that tumors originating from CSCs mimicked actual human colon cancer tissues. Indeed, while HCT116 cells give rise to tumors composed by solid sheets of poorly differentiated epithelial cells, colon CSC-derived tumors grow in well-differentiated glandular structures composed by large epithelial cells clustering around irregular gland lumen containing mucin and cells debris. Histograms show the mean values ±SD of three independent experiments.

**A**

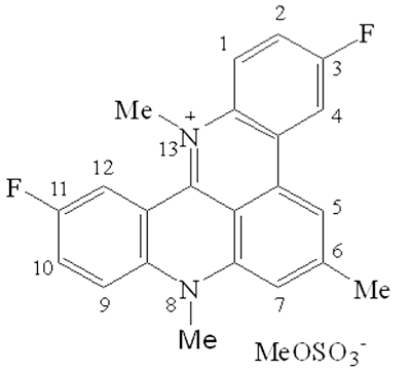


RHPS4

**B**

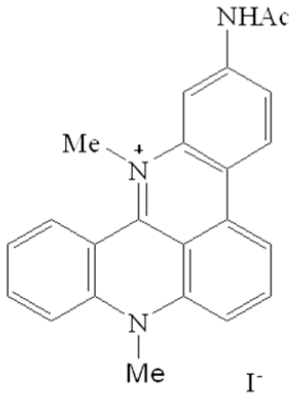


RHPS4$_{der1}$

**C**

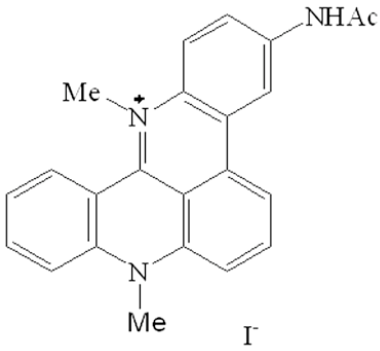


RHPS4$_{der2}$

**D**

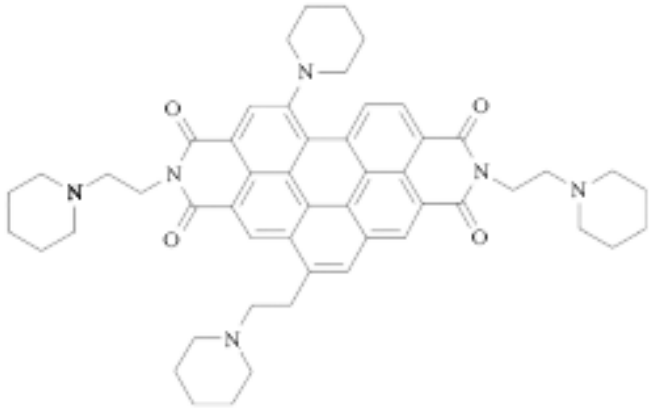


Emicoron

**Supplemental Figure S2.** Structure of used G4 ligands. **A** pentacyclic acridinium salt RHPS4 (3,11-difluoro-6,8,13-trimethyl-8H-quino [4,3,2-kl] acridinium methosulfate). **B** RHPS4-derivative 1 (RHPS4$_{der1}$, 2-acetylamino-8,13-dimethyl-8H-quino[4,3,2-kl]-acridinium iodide). **C** RHPS4-derivative 2 (RHPS4$_{der2}$, 3-acetylamino-8,13-dimethyl-8H-quino[4,3,2-kl]-acridinium iodide). **D** Emicoron (N,N'-bis[2-(1-piperidino)-ethyl]-1-(1-piperidinyl)-6-[2-(1-piperidino)-ethyl]-benzo[ghi]perylene-3,4:9,10-tetracarboxylic diimide).

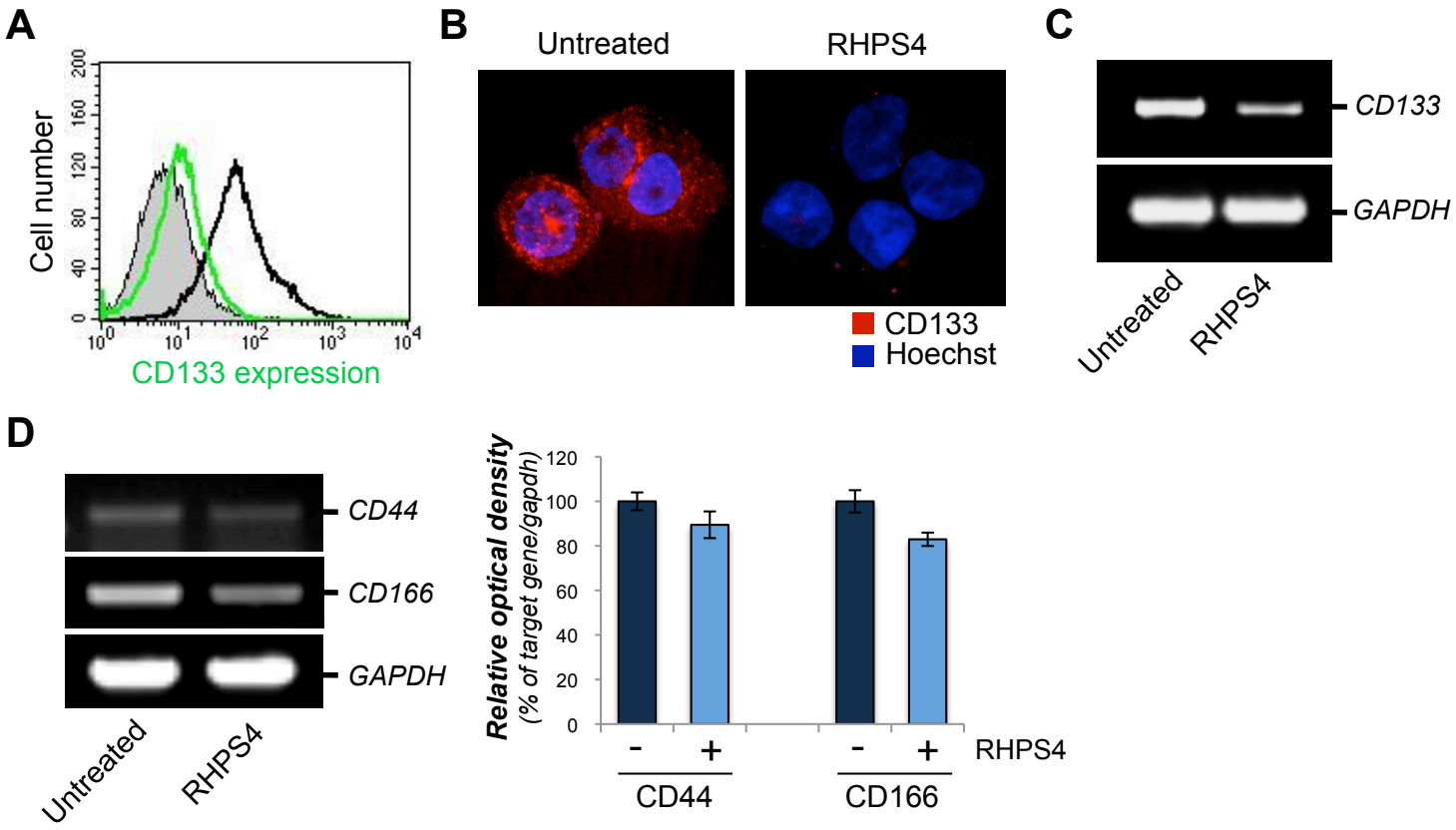


**Supplemental Figure S3.** Expression of CSC marker CD133 is selectively impaired by treatment with RHPS4. **A** CSC_2 cells, untreated or treated with 1 μM RHPS4 for 96 hrs, were immunostained with an anti-CD133 antibody and processed for FACS analysis. The histogram shows the fluorescence intensities in the negative control (grey area), untreated (black line) and treated (green line) samples. **B** CSC_2 cells were treated as in A and the expression CD133 was analysed by IF microscopy. Representative IF pictures show CD133 staining (red) merged with Hoechst (blue) under the indicated conditions (63X magnification). **C** RT-PCR analysis of *CD133* expression in CSC_2 cells. Picture shows the PCR amplification products run on agarose gel. Expression levels of *GAPDH* were evaluated as loading control. **D** CSC_1 cells were grown for 96 hrs in absence or in presence of 1μM RHPS4 and gene expression of the stemness markers CD44 and CD166 was analysed by RT-PCR. The picture shows the PCR amplification products run on agarose gel. Expression levels of *GAPDH* were evaluated as loading control. The histogram shows the relative optical density of *CD44 and CD166*.

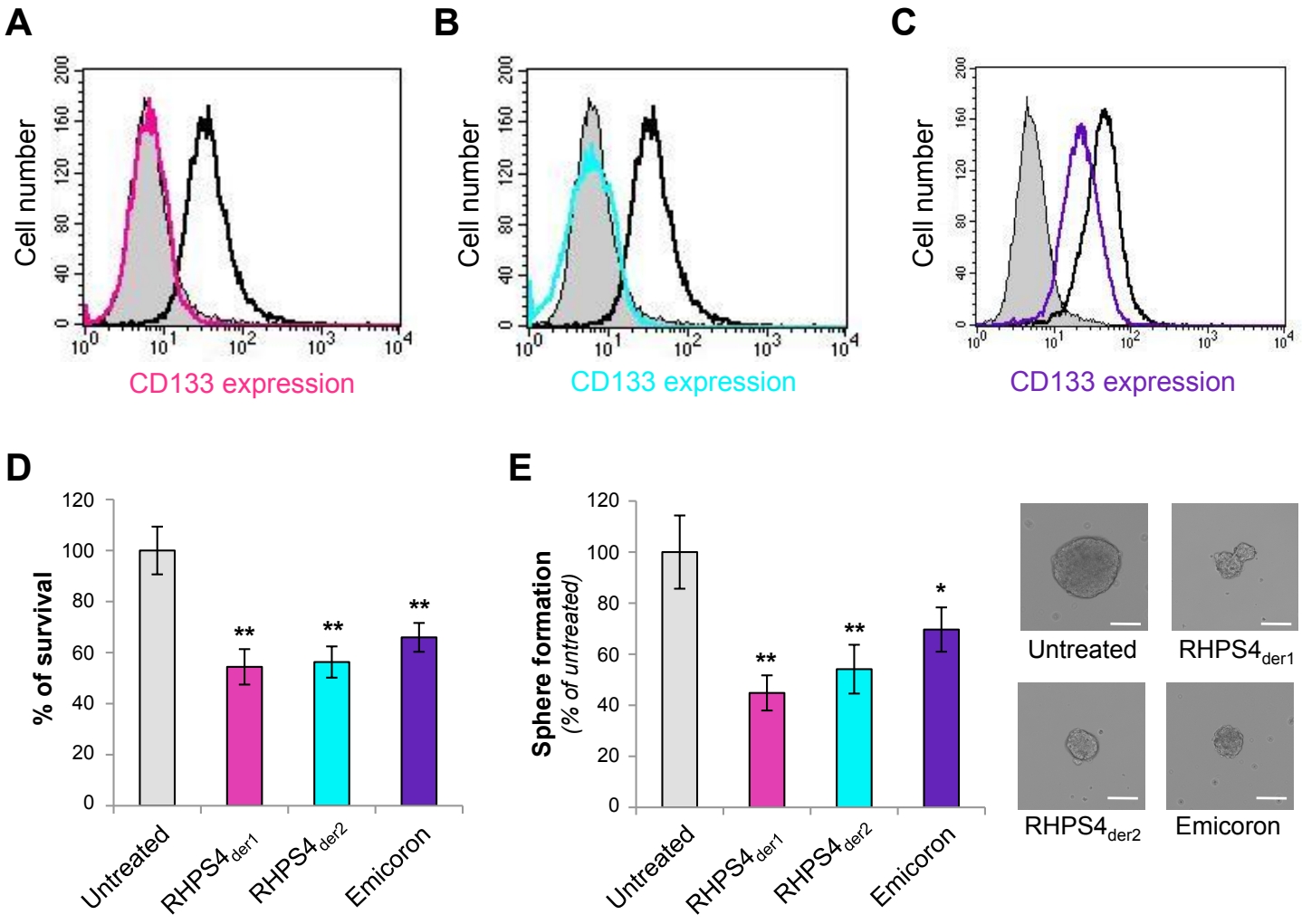


**Supplemental Figure S4.** G4 ligands impair CSC features by affecting the expression of CD133. **A-C** CSC_1 cells, untreated or treated for 96 hrs with **A** 1 μM of RHPS4-derivative 1 ($RHPS4_{der1}$), **B** 1 μM of RHPS4-derivative 2 ($RHPS4_{der1}$) or **C** 0.5 μM of Emicoron, were immunostained with an anti-CD133 antibody and processed for FACS analysis. The histograms show the fluorescence intensities in the negative controls (grey areas), untreated (black lines) and treated (colored lines) samples. Histograms show one representative of three independent experiments with similar results. **D** CSC_1 cells were treated for 96 hrs with RHPS4-derivative 1 ($RHPS4_{der1}$, 1 μM), RHPS4-derivative 2 ($RHPS4_{der2}$, 1 μM), or Emicoron (0.5 μM), and colony forming ability was evaluated. The graph shows the surviving fractions calculated as the ratio of absolute survival of the treated/ untreated samples (**= p<0.01). **E** Primary tumorspheres, untreated or treated as in D, with the indicated G4 ligands, were dissociated and the cell ability of originating secondary spheres was evaluated. The histogram shows the percentage of secondary tumorspheres obtained 5 days after dissociation (*= p<0.1 **= p<0.01). For each condition a representative image of secondary tumorspheres is reported.

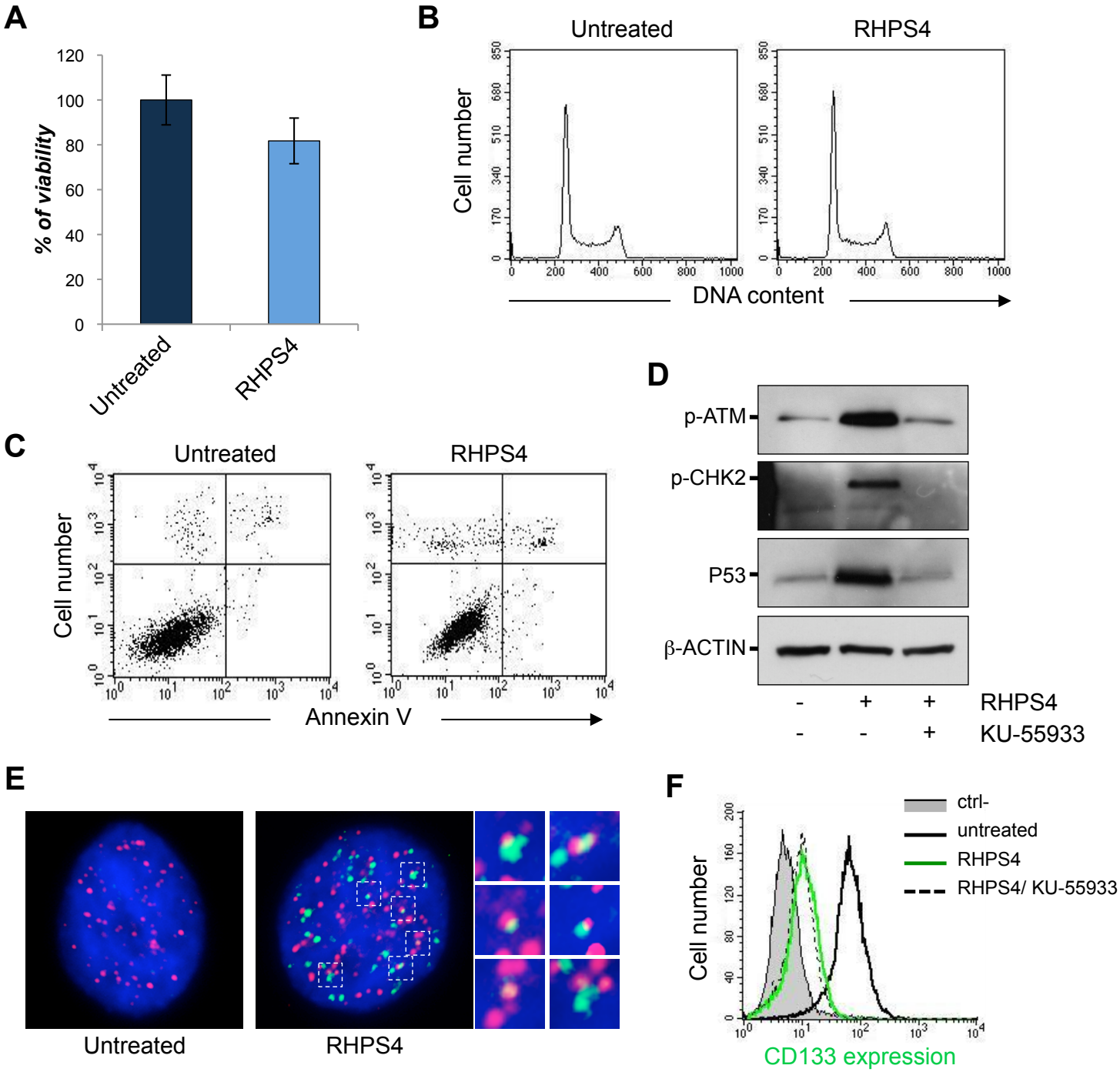


**Supplemental Figure S5.** G4 ligands do not affect CSCs viability and their effect is independent from the DNA damage. **A** Colon CSCs (CSC_1) were grown for 96 hrs in absence (untreated) or in presence of 1 μM RHPS4 and cell viability was evaluated by MTT assay (Sigma-Aldrich, 5 mg/mL in phosphate-buffered saline). Histograms represent the percentage of viable cells. **B and C** CSC_1 cells treated as in A were processed for FACS analysis to evaluate **B** cell cycle by PI staining and **C** apoptosis by annexin V expression. **D** CSC_1 cells were treated as indicated in the figure and the activation state of DNA damage response proteins was analysed by western blotting analysis using the following antibodies: rabbit mAb anti-Ser1981 p-ATM; mouse mAb anti-p53 DO-1 and rabbit pAb anti-Thr68 p-CHK2. As loading control, levels of β-ACTIN were evaluated by using the mouse mAb anti-β-actin. **E** CSC_1 were grown in absence (untreated) or in presence of 1 μM of RHPS4 and then processed for IF microscopy analysis by using antibodies against γH2AX and TRF1 to mark DNA damage and telomeres, respectively. Hoechst staining was used to mark nuclei. Representative images (magnification 100X) are shown. Enlarged views (2.5X) of telomere-induced foci (TIF) are also shown. **F** CSC_1, treated as in D were immunostained with an anti-CD133 antibody and processed for FACS analysis. Histograms refer to the means ±SD of three independent experiments.